Experimental Evaluation of Asphalt Concrete Interlayer Shear Strength: Role of Thermal, Bonding, and Structural Factors

Ali Dehghani[1], Mahdi Shojaei[2], and Fereidoon Moghadas Nejad[3*]

[1]Graduate Student, Dept. of Civil and Environmental Engineering, Amirkabir University of Technology, Tehran, Iran.
[2]Research Assistant, Dept. of Civil and Environmental Engineering, Amirkabir University of Technology, Tehran, Iran.
[3]Professor, Dept. of Civil and Environmental Engineering, Amirkabir University of Technology, Tehran, Iran.

Abstract

Bonding characteristics between asphalt concrete layers have been a major concern for decades, as poor adhesion can lead to premature pavement distress, including cracking and fatigue. Hence, this study investigates the individual and interactive effects of temperature, tack coat application rate, confinement load, aggregate interlock, surface preheating, and geocomposite reinforcement on interlayer shear strength. The results showed that temperature is the most detrimental factor, reducing the strength overall by more than 2.5 times as it increased from 10°C to 40°C. Meanwhile, confinement load and aggregate interlock are the most important contributors to strength. Applying a 100 kPa confinement pressure boosted average strength by 60%, and aggregate interlock increased strength by 28% at high temperatures. Furthermore, statistical analysis revealed that surface preheating has no significant impact on the final strength. Importantly, critical interactions between confinement load and tack coat rate, as well as a negative interaction between aggregate interlock and the geocomposite, were recognised. Specifically, while aggregate interlock significantly increased strength by 28% at 40°C, the addition of geocomposites introduced a negative interaction, reducing the shear strength by approximately 17%. This finding quantifies the trade-off, demonstrating that geocomposites can partially negate the mechanical benefits of interlock. These results provide a robust framework for optimising pavement design by prioritising synergistic factor combinations.

Keywords:

Asphalt overlay, tack coat, interlayer shear strength, shear bonding, double-shear test

* Corresponding author. Email: moghadas@aut.ac.ir

1 Introduction

Pavement structure usually consists of several layers, including asphalt concrete (AC), base, subbase, and subgrade bonded with bituminous materials. In this regard, several studies have reported that the bonding state at each interface plays a crucial role in determining the stress distribution within a pavement structure. Insufficient bonding at the topmost interface can disrupt the efficient transfer of loads across the pavement structure. This unbalanced load distribution leads to excessive stress on the AC layer, making it more susceptible to different distresses, including slippage cracking, top-down cracking, and fatigue cracking, which ultimately reduces the pavement service life up to 25–50 % [1–8]. A preventive measure is applying a thin layer of bituminous material named tack coat to not only ensure bonding and enhance adhesion between AC layers but also improve its structural integrity and extend pavement service life [9].

Generally, the performance of the tack coat binder depends on several factors, especially traffic, environmental conditions, binder quality and quantity, and bonding conditions. For instance, the application of PG 64-22, PG 76-22M binder, and four types of emulsion was evaluated, and researchers concluded that there is a significant drop in Interface Shear Strength (ISS) with increasing temperature [10]. In another study, Hu et al. investigated the impact of temperature, tack coat dosage, and tack coat type on ISS under monotonic loading. Results not only confirmed that the rise of temperature leads to a reduction of ISS but also revealed that the reduction rate gradually diminished [11]. Moreover, it is noted that ISS increases with the amount of tack coat applied. However, excessive usage causes a drop in strength [11,12]. It is also documented that increasing anionic slow-setting and cationic rapid-setting tack coats resulted in a steady decrease in ISS values. In contrast, hard base binder tack coats displayed an upward trend in ISS values as application rates rose [13].

In addition, rheological properties and tack coat type are reported to play vital roles in ISS and the optimum tack coat [14,15]. Researchers even concluded that the tack coat type has more impact than the application rate [16]. In another study, the rheological parameters of a cationic rapid-setting and a polymer-modified emulsion with a hard base asphalt binder were evaluated at different temperatures to relate to the ISS values of field core samples. The results show that when the $G^*/\sin\delta$ value (the binder anti-rutting indicator of the Superpave binder specification system) increased, the ISS values rose regardless of the application rate. However, as the $G^*/\sin\delta$ values increased, the differences in ISS values between application rates became more noticeable, specifically for the modified emulsion [17].

In this line of research, Noory et al. examined the effect of temperature and geocomposite on the shear bonding between AC layers. They also reported the adverse impact of temperature on cohesion and shear bonding between layers. Moreover, a general decrease in ISS was observed in reinforced samples, with the extent of this reduction attributed to the composition of the reinforcements. It was also found that a larger grid size enhanced shear bonding by promoting more effective interlocking between aggregates [18]. However, another study found that ISS increased with grid size up to an optimal mesh opening of 900 mm^2, after which it decreased as the grid size continued to increase. It has also been specified that the material composition of geosynthetics can contribute to ISS [19,20]. It is worth noting that the role of geocomposites in interlayer performance is multifaceted and involves trade-offs. While some studies reported a reduction in ISS, a substantial body of research focusing on pavement fatigue life highlighted its primary engineering function [21–23]. This improvement is attributed to the geocomposite's ability to absorb and redistribute tensile stresses at crack tips, thereby retarding reflective cracking.

Regarding traffic impacts, scholars evaluated how normal stress on samples affects ISS and demonstrated that applying higher normal stress increases shear strength due to increased friction and adhesion between AC layers [6,24]. Furthermore, the effect of different surface characteristics was

evaluated, and it was emphasised that as the contact points between two AC layers decreased, the peak shear strength also diminished [24,25]. Besides, findings from a field study confirmed that milled surfaces had substantially greater bond strength compared to non-milled surfaces [26]. Similarly, Covey et al. demonstrated a strong positive correlation between pavement surface texture and ISS. They reported that rough surfaces offer increased mechanical interlock and enhance the adhesion between layers when a tack coat is applied [14].

In summary, many studies have concluded that tack coat plays a crucial role in enhancing pavement durability by focusing on its effect on AC interlayer bonding properties and highlighting other influential factors. However, most previous studies have been limited to examining one or two parameters in isolation. Despite these contributions, a significant research gap remains. The existing body of knowledge often neglects the complex, simultaneous interactions within pavement structures. Specifically, there is a lack of quantitative understanding of how structural factors, such as aggregate interlock and geocomposite reinforcement, interact with environmental conditions and construction variables, such as tack coat rate. Without determining these interactions, it is impossible to accurately predict the performance of an interlayer system.

Therefore, this study aims to go beyond single-factor analysis and provide a more integrated understanding of interlayer behaviour and determine how ISS is influenced by the interactions of factors, including temperature, tack coat application rate, geocomposite, confinement load, preheating, and aggregate interlock. Additionally, by utilising statistical analysis, this paper will provide further insight into the impact of variables on shear strength and offer better solutions to improve pavement durability.

2 Material and experimental program

2.1 Materials

A limestone quarry in Tehran City, Iran, supplied the crushed aggregate used in this study. Fig. 1 shows the gradation of utilised aggregates. Furthermore, the most common and available binder in Iran, PG 64-22, was used to prepare asphalt mixtures. The results of conventional tests of this binder are summarised in Table 1. To ensure experimental consistency and isolate the effects of the six primary factors under investigation, the study employed a single type of tack coat and geocomposite. Using only one tack coat eliminated potential confounding variables linked to differences in asphalt emulsion formulations, such as breaking time, water content, and emulsifier chemistry. The selected tack coat was a standard paving grade bitumen with a penetration of 76, commonly used in Iran. Similarly, a glass grid bonded to a non-woven polypropylene fabric was chosen for its typical application. Table 2 also provides the properties of geosynthetic.

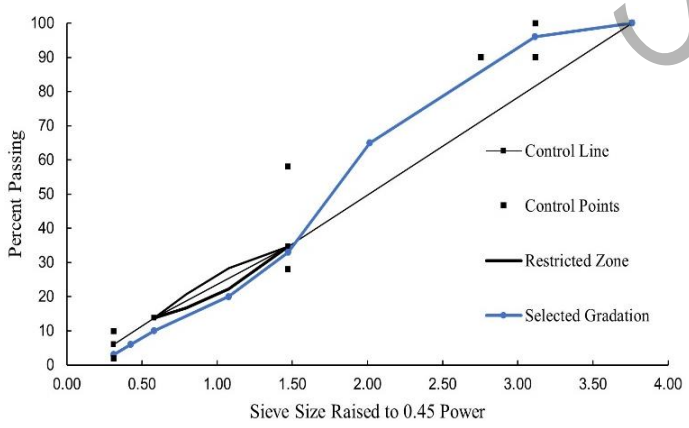

Fig. 1. Aggregate gradation curve of the asphalt mixture

Table 1- Conventional properties of the asphalt binder

Property	Result
Penetration (1/10 mm)	70
Ductility @ 25°C (cm)	120
Ductility @ 5°C (cm)	4
Softening point (°C)	54.6

Table 2- Properties of the geosynthetic

Property	Unit	Result
Tensile strength of composite	kN/m	100
Tensile strength of geotextile	kN/m	9
Effective mesh size	mm	33
Elongation at break	%	3
Bitumen retention	kg/m2	1.1
Mass per unit area	g/m2	581

2.2 Experimental methods and AUT-SLT apparatus

Bonding characteristics between AC layers have been a concern of researchers for the past few decades, prompting the development of several laboratory apparatuses based on shear test, torque test, and tensile tests to measure bonding strength [16,27,28]. It is reported that shear testing is the most frequently employed method for analysing bond characteristics [16]. Some shear testing methods include the Leutner shear tester, layered parallel direct shear test, Florida direct shear test, Ancona shear testing research and analysis device, Louisiana interlayer shear test, double shear test, and large-scale interface shear strength test [16,20]. Among these tests, the double shear test, developed by Diakhaté et al., enables the measurement of shear strength and the analysis of interface behaviour between different asphalt layers by applying shear loads to two AC specimens [2].

Noory et al. introduced a modified double shear test named Amirkabir University of Technology Shear Lab Tester (AUT-SLT) that can apply the shear load and normal load caused by the vehicle's weight simultaneously, unlike conventional monotonic shear tests that often lack confinement capabilities to accurately investigate interlayer properties [18]. AUT-SLT consists of multiple parts and allows shear loading. As depicted and well-documented by Noory et al., the specimens should be positioned within the three clamps so that the interlayer is placed next to the gap between the two clamps [29]. This zone is known as the interlayer shear zone.

With this setup, the vertical shear load is applied by the UTM actuator's load cell, and the shear displacement is measured using a Linear Variable Differential Transformer (LVDT) mounted on the fixed frame, with its sensing core in contact with the moving central clamp. Meanwhile, the lateral confinement force is monitored to ensure stability. This arrangement allows for the direct recording of the relative slip between the asphalt layers. Clearly, while two clamps remain fixed, the middle clamp moves vertically, and four linear ball bearings and rails restrict its movement in the other directions. Fig. 2 shows the schematic diagram and a picture of the experimental setup.

Also, Noory et al. conducted a laboratory simulation of a pavement structure to establish a representative displacement rate for the test protocol. They measured the shear displacement between the overlay and underlying asphalt pavement using a linear variable differential transformer. Plotting displacement versus loading time showed that the slope of the curve became constant in certain regions, indicating a steady displacement rate. Therefore, a displacement rate of 12.5 mm/min for the movable clamp is recommended to simulate the observed field behaviour accurately [18]. It is worth noting that the validation of the AUT-SLT device and its capability to simulate field failure mechanisms have been proven in previous studies [18,29,30]. Therefore, detailed validation procedures are not repeated here. This study used the AUT-SLT device to measure the shear strength between AC layers.

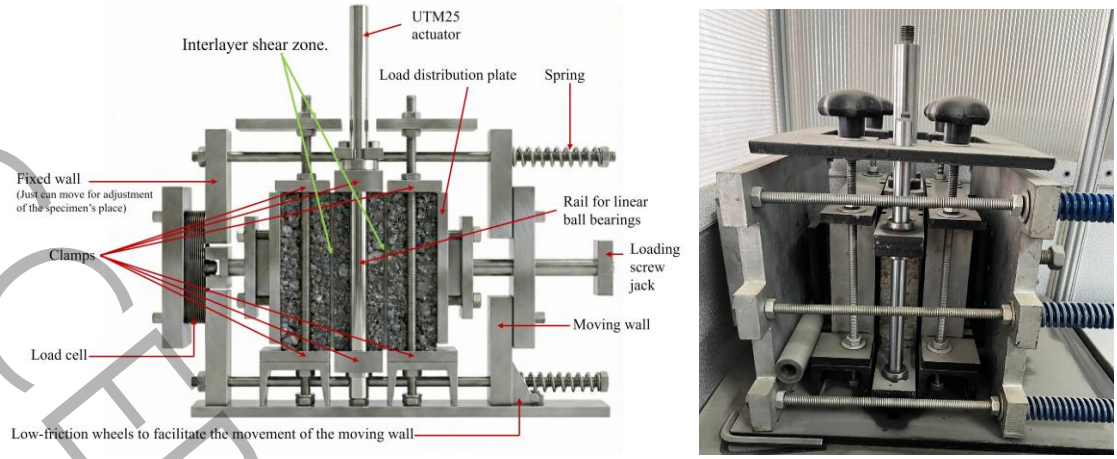

(a) (b)

Fig. 2. (a) Schematic diagram and (b) picture of the AUT-SLT device

2.3 Mixture design and sample preparation

The sample preparation in this study consisted of four stages. 1) The optimum binder content of mixtures with 4% air void was obtained at 4.85% by implementing the Marshall mixture design approach. 2) Cubic-shaped samples were prepared in a shear compactor, PReSBOX, which can simulate the field-compaction status because of the pressure and shear cycles. Samples were compacted to 150 mm by 150 mm by 450 mm, and then two slab samples, 50 mm by 150 mm by 450 mm, were cut from the core. These two samples were used as side support layers in a double shear test device. 3) In this stage, one of the support layers from stage two was placed in the mould of the PReSBOX compactor. After applying the interlayer condition(s) to the support asphalt slab, a specified amount of loose hot asphalt mixture was poured onto it at 120°C to form the central layer. Finally, the second slab with the identical interlayer condition was placed on top of the mixture, completing the sandwich structure. This assembly was then compacted until the central layer reached a target air void of 4%, ensuring uniformity with the properties of the outer support layers. 4) After reaching room temperature, the final three-layered specimen was removed from the compactor and divided into three cubic testing specimens with dimensions of 150 mm by 150 mm by 150 mm.

Fig. 3 (a) shows a compacted sample in the PReSBOX device and Fig. 3 (b) a sliced specimen ready for applying the interlayer condition. The final specimens were conditioned in a temperature chamber for 12 hours to ensure they reached the test temperature.

2.4 Experimental program

An experimental program was designed to examine the impacts of temperature, geocomposite, confinement load, preheating, aggregate interlocking, and tack coat application rate on interface shear bond strength. Table 3 presents the experimental matrix, which includes two levels for each influential factor. In total, 64 interlayer conditions were evaluated, and three replicates for each condition were subjected to interface shear tests.

As can be seen from Table 3, two temperatures of 10°C to 40°C, confinement loads of 0 kg and 229 kg (approximately 100 kPa), and residual application rates of 0.5 Kg/m^2 and 1 Kg/m^2, uniformly distributed with 100% coverage, were considered in this study. The HMA surface was dry and clean before applying the tack coat. The effects of the other three variables, including aggregate interlock, surface preheating, and geocomposite, were evaluated in terms of their presence and absence. The preheating process was carried out by subjecting the lateral layers to a temperature chamber at 50°C for one hour. Choosing 10°C and 40°C as the low and high temperature levels was not meant to replicate the single coldest and hottest hours of the year. Instead, it was based on representative points along the

performance temperature, which are critical for evaluating ISS. Selecting 40°C is to test within a temperature range where the selected binder's viscosity becomes predominant and poses a risk to the structural integrity of the pavement interlayer. Conversely, the 10°C test temperature was chosen to represent the elastic-dominant condition rather than an extreme cold-weather scenario.

Table 3- Laboratory test factorial in this study

Variable	Code	Unit	Level	
			1	2
Temperature	A	℃	10	40
Confinement load	B	kg	0	229
Tack coat application rate	C	Kg/m2	0.5	1
Surface preheating	D	-	Without preheating	With preheating
Aggregate interlock	E	-	Without interlock	With interlock
Geocomposite	F	-	Without geocomposite	With geocomposite

(a) (b)

Fig. 3. (a) Compacted sample. (b) Sliced sample

3 Results and discussion

Table 4 and Table 5 show the average value of peak shear strength between layers of all interlayer conditions at temperatures of 10°C to 40°C, respectively. While it is necessary to assess the main effects of key variables such as temperature and tack coat application rate, neglecting interaction effects can result in an incomplete understanding and oversimplifying the behaviour of AC shear resistance. Therefore, the following aims to discuss findings by examining the main and interaction effects.

3.1 Experimental results

The average value of ISS at 10°C and 40°C, considering three categorical variables of surface preheating, aggregate interlock, and geocomposite, is depicted in Fig. 4. It reveals that increasing the temperature to 40°C reduced the overall average strength by more than 2.5 times. This inverse relationship is attributed to the rheological behaviour of bitumen, which softens at elevated temperatures. At 10°C, it provides strong cohesive strength and efficiently resists the applied shear forces. As the temperature rises to 40°C, the binder undergoes a significant viscoelastic transition. As the stiffness of bitumen decreases, its binding capability diminishes, resulting in a lower resilient modulus and, consequently, reduced shear strength [31].

Table 4- The ISS values of all interlayer conditions at 10°C

No.	Variables					Strength kN/m2
	B	C	D	E	F	
1	B1	C1	D1	E1	F1	420.7531
2	B1	C1	D2	E1	F1	421.6773
3	B1	C1	D1	E2	F1	442.3951
4	B1	C1	D2	E2	F1	471.764
5	B2	C1	D1	E1	F1	550.7238
6	B2	C1	D2	E1	F1	624.2325
7	B2	C1	D1	E2	F1	630.0283
8	B2	C1	D2	E2	F1	594.2895
9	B1	C1	D1	E1	F2	439.9689
10	B1	C1	D2	E1	F2	424.6182
11	B1	C1	D1	E2	F2	516.2921
12	B1	C1	D2	E2	F2	462.969
13	B2	C1	D1	E1	F2	566.4522
14	B2	C1	D2	E1	F2	561.3224
15	B2	C1	D1	E2	F2	560.0803
16	B2	C1	D2	E2	F2	586.3667
17	B1	C2	D1	E1	F1	398.7136
18	B1	C2	D2	E1	F1	435.5177
19	B1	C2	D1	E2	F1	473.7134
20	B1	C2	D2	E2	F1	516.135
21	B2	C2	D1	E1	F1	609.9184
22	B2	C2	D2	E1	F1	613.0705
23	B2	C2	D1	E2	F1	678.9252
24	B2	C2	D2	E2	F1	688.0171
25	B1	C2	D1	E1	F2	450.7268
26	B1	C2	D2	E1	F2	475.4059
27	B1	C2	D1	E2	F2	401.3043
28	B1	C2	D2	E2	F2	447.0002
29	B2	C2	D1	E1	F2	594.5465
30	B2	C2	D2	E1	F2	686.1129
31	B2	C2	D1	E2	F2	650.3826
32	B2	C2	D2	E2	F2	609.0837

Table 5- The ISS values of all interlayer conditions at 40°C

No.	Variables					Strength kN/m2
	B	C	D	E	F	
33	B1	C1	D1	E1	F1	68.2414
34	B1	C1	D2	E1	F1	78.95534
35	B1	C1	D1	E2	F1	43.564
36	B1	C1	D2	E2	F1	169.2111
37	B2	C1	D1	E1	F1	212.1112
38	B2	C1	D2	E1	F1	229.2875
39	B2	C1	D1	E2	F1	317.1587
40	B2	C1	D2	E2	F1	322.685
41	B1	C1	D1	E1	F2	43.24863
42	B1	C1	D2	E1	F2	100.5315
43	B1	C1	D1	E2	F2	96.57842
44	B1	C1	D2	E2	F2	65.98496
45	B2	C1	D1	E1	F2	215.1949
46	B2	C1	D2	E1	F2	248.6905
47	B2	C1	D1	E2	F2	179.5277
48	B2	C1	D2	E2	F2	301.118
49	B1	C2	D1	E1	F1	139.277
50	B1	C2	D2	E1	F1	103.2632
51	B1	C2	D1	E2	F1	125.4669
52	B1	C2	D2	E2	F1	172.1021
53	B2	C2	D1	E1	F1	348.4159
54	B2	C2	D2	E1	F1	267.1328
55	B2	C2	D1	E2	F1	350.0796
56	B2	C2	D2	E2	F1	288.1517
57	B1	C2	D1	E1	F2	57.2725
58	B1	C2	D2	E1	F2	102.5898
59	B1	C2	D1	E2	F2	116.7328
60	B1	C2	D2	E2	F2	145.0968
61	B2	C2	D1	E1	F2	233.8526
62	B2	C2	D2	E1	F2	199.5172
63	B2	C2	D1	E2	F2	304.6335
64	B2	C2	D2	E2	F2	286.3503

According to the data, the variation in ISS at 10°C and 40°C differed depending on the interlayer condition. For example, applying preheating and interlock conditions at 10°C increased strength by 2.8% and 5.5%, respectively, and using the geocomposite reduced it by 1.6%. Meanwhile, these variations became pronounced at 40°C, with preheating and interlock increasing strength by 8% and 28%, respectively, while using the geocomposite decreased it by 16.7%. It can be concluded that the ISS values at high temperatures are more associated with interlayer conditions than at lower temperatures. Additionally, the notable impact of aggregate interlock on strength, increasing ISS by 28% at 40°C, highlights its role in maintaining interlayer integrity at high temperatures. In other words, the physical interlock mechanism provides a robust resistance to shear that is less sensitive to thermal softening than the tack coat's adhesion.

As shown in Fig. 4, preheating negligibly improved ISS. This may be explained by the overwhelming thermal dominance of the hot mix asphalt overlay and the inherent thermal properties of the existing asphalt layer. In this study, the interlayer mixture was placed at 120°C, whereas the support layer was either at ambient temperature or preheated to 50°C. Upon contact, the cooler mass of the support layer acts as a heatsink, but the interface temperature is overwhelmingly dictated by the 120°C overlay. The tack coat at the interface is instantaneously heated to a temperature far exceeding the 50°C preheating temperature, causing a rapid and significant drop in its viscosity. This effect occurs in both the preheated and non-preheated scenarios. In other words, the initial temperature difference between a preheated and non-preheated surface becomes negligible in the final thermal equilibrium achieved at the interface during compaction.

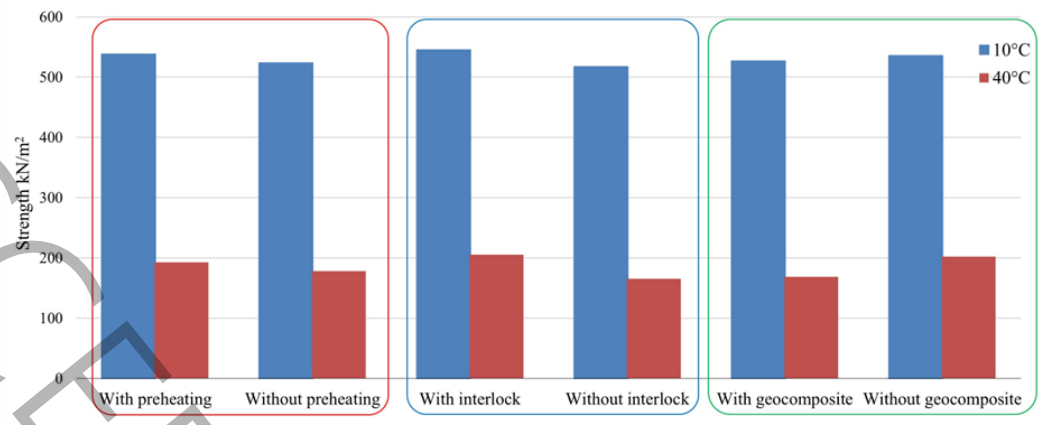

Fig. 4. Average value of ISS at 10°C and 40°C

The influence of confinement load on ISS was also analysed to understand both its overall impact and its interaction with temperature. As depicted in Fig. 5 (a), applying a confinement load of 229 kg enhanced the interface performance, resulting in a 60% increase in average ISS compared to the unconfined condition. This overall improvement stems from greater frictional resistance and interlocking at the interface. However, as illustrated in Fig. 5 (b), the magnitude of this benefit is highly dependent on the thermal condition. While increasing the temperature from 10°C to 40°C caused a drastic 75% loss in shear strength under no confinement, the application of the 229 kg load mitigated this reduction to approximately 55%. This comparison highlights a shift in the dominant resisting mechanism. At low temperatures, where the tack coat binder is stiff and contributes significantly to shear resistance, the addition of confinement load provides a moderate increase in strength. In contrast, at 40°C, where the binder has softened, and its adhesive contribution is minimal, the benefit of confinement load is maximised.

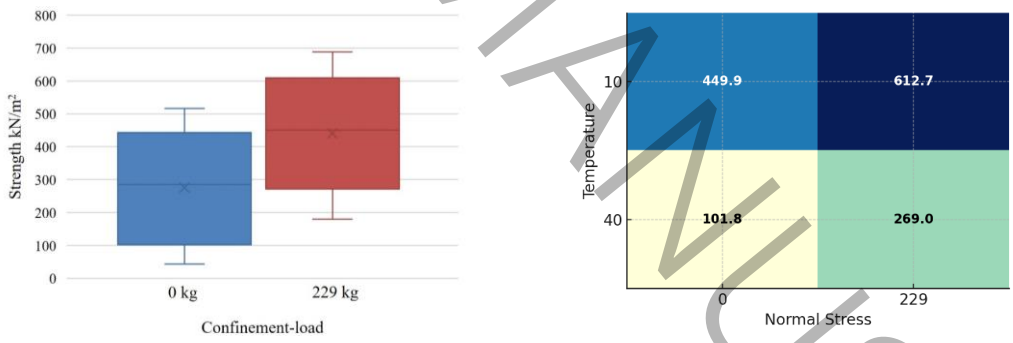

(a) (b)

Fig. 5. (a) Effect of confinement load on ISS with different interlayer conditions. (b) Heatmap of average strength by temperature and confinement load

The overall effect of the tack coat application rate was evaluated under varying interlayer conditions. As demonstrated in Fig. 6, increasing the tack coat rate from 0.5 kg/m² to 1.0 kg/m² consistently resulted in higher ISS values. This trend underscores the crucial role of the tack coat in strengthening the bond between asphalt layers. This influence and the relative improvement in ISS with an increase in tack coat were particularly pronounced in the control configuration, where no preheating, interlock, or geocomposite is applied. The control configuration is specified by the green boundary in Fig. 6. The reason for this pronounced effect is that in the control configuration, the interlayer shear resistance is almost exclusively dependent on the chemical adhesion provided by the tack coat, and in the absence of supplementary mechanical contributions, the role of tack coat as the primary bonding agent is magnified. Consequently, any enhancement to this sole mechanism (in this case, increasing the

application rate from 0.5 to 1.0 kg/m²) results in a more significant and direct improvement in the total measured ISS.

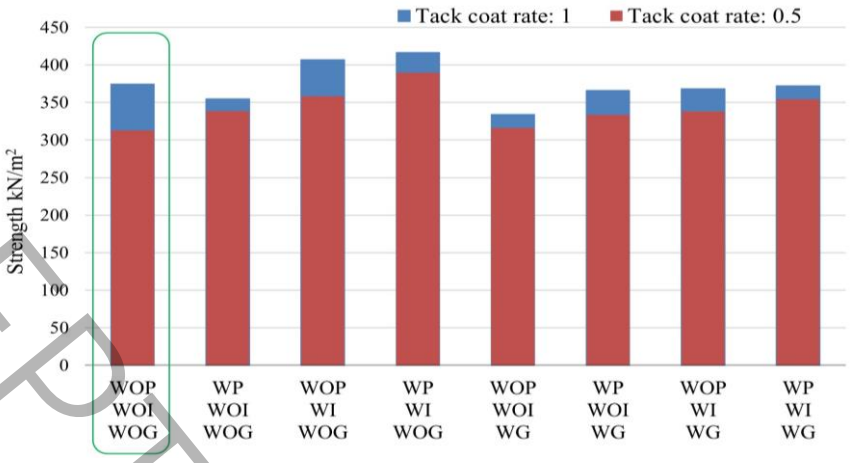

WP: With Preheating, WOP: Without Preheating, WI: With Interlock, WOI: Without Interlock, WG: With Geocomposite, WOG: Without Geocomposite.

Fig. 6. Effect of tack coat application rates on ISS with different interlayer conditions

Furthermore, a quantitative analysis of the data showed that the marginal benefit of increasing the tack coat rate diminishes at lower temperatures. At 10°C, increasing the tack coat amount results in only a 5% increase in the average ISS, while at 40°C the same increase in the tack coat yields a substantial 21% improvement in ISS. This observation highlights a possible interaction between temperature and tack coat content, underscoring the need to consider ambient temperature when determining the optimal tack coat amount.

It is also observed that the application of a geocomposite generally results in a lower ISS than its non-geocomposite counterpart under most conditions, suggesting a debonding effect introduced by the reinforcement layer. This might be justified by the fact that the presence of a geocomposite can act as a physical barrier between the asphalt layers, impeding direct aggregate-to-aggregate contact and leading to layers sliding over each other. However, a notable exception to this trend is observed in the structure that was preheated but had no aggregate interlock. In this specific scenario, when the higher tack coat rate of 1.0 kg/m² is applied, the geocomposite-reinforced sample (WP, WOI, WG) exhibits a slightly greater shear strength than the unreinforced equivalent (WP, WOI, WOG), indicating a potential synergistic interaction.

Results suggest a key strategic consideration for pavement design. When a geocomposite is needed for its functional advantages, such as slowing crack growth, the best way to offset the loss of shear strength is to use other strengthening strategies simultaneously, such as creating aggregate interlock and preheating. For example, the sample with geocomposite, preheating, and aggregate interlock achieves a higher ISS than the control case. This demonstrates that mechanical enhancements can effectively offset the geocomposite's negative impact on strength. But the effectiveness of this approach strongly depends on the tack coat quantity. At the higher tack coat rate, a close analysis of Fig. 6 reveals that, even when the geocomposite is combined with all other enhancements, ISS remains equal to the strength of the unreinforced control sample. This indicates that at high tack coat rates, the geocomposite's debonding effect is difficult to fully overcome. Conversely, a more favourable trend emerges at the lower tack coat rate of 0.5 kg/m².

In this scenario, combining the geocomposite with other strengthening strategies yields an ISS value notably higher than that of the corresponding unreinforced control sample. This suggests that at lower tack coat rates, the mechanical enhancements work more synergistically with the geocomposite.

These findings underscore the importance of not only selecting interlayer materials but also ensuring they are implemented within a comprehensive framework that includes an appropriate tack coat rate and surface preparation techniques. Simply adding a geocomposite without considering these interacting factors may lead to suboptimal or even counterproductive results.

3.2 Statistical analysis

The abovementioned experimental results and visual inspection of the data indicated a complex, multi-factorial relationship between interlayer conditions and ISS. Therefore, a simple linear model, which assumes each factor's contribution is constant and independent, would fail to capture this complex behaviour. Hence, to develop a predictive model, a comprehensive statistical analysis was undertaken. The objective was to move beyond a simple assessment of main effects and to critically evaluate the significance of two-way interaction terms. Throughout this analysis, a significance level of $\alpha = 0.05$ was established as the criterion for statistical significance and variable selection.

To systematically identify all significant relationships, a complete factorial regression model was initially developed. This comprehensive initial model included all six main factors investigated in this study as well as all possible two-way interaction terms, resulting in a total of 21 potential predictors. Such a large model suffers from two key issues. Firstly, the inclusion of many statistically insignificant terms adds noise and reduces predictive precision. Secondly, multicollinearity or highly intercorrelated variables make the model's coefficients unstable to interpret. To address these issues, a systematic backward elimination process was used, which is a standard statistical method for refining models.

The process involves fitting the model with all predictors, then identifying the predictor with the highest p-value. If this p-value exceeds 0.05, the predictor is removed. The model is refitted with the remaining predictors, and this process is repeated until all predictors have p-values of 0.05 or less. This approach ensures that the final model only includes factors and interactions that are statistically significant for ISS. In this study, the backward elimination procedure was executed over 16 iterations, reducing the number of predictors from 21 to 5. The initial and optimised models are summarised in Table 6 and Table 7, respectively. Table 7 demonstrates an excellent fit by explaining 97.0% of the variance in ISS ($R^2 = 0.970$). The high F-statistic (380.1) and its associated low probability value ($p < 0.001$) indicate that the overall model is highly significant. The final predictive equation derived from this analysis is presented by Equation (1).

$$ISS = 547.08 - 11.53 \times T + 0.43 \times CL + 51.44 \times AI + 0.387 \times CL \times TCR - 34.64 \times AI \times G \quad (1)$$

where ISS is interlayer shear strength (kPa), T is the temperature (°C), CL is the confinement load (kg), TCR is the tack coat application rate (kg/m^2), and AI and G are binary variables equal to 1 if aggregate interlock and geocomposite are present, respectively, and 0 otherwise.

The optimised model reveals several key insights that align with experimental observations. As shown in Table 7, temperature emerges as an influential factor affecting ISS. The negative coefficient of -11.53 aligns perfectly with the expected behaviour of asphalt binder, which softens at higher temperatures, reducing its adhesive and cohesive strength. Also, it shows that aggregate interlock has a substantial positive effect and quantifies the critical role of mechanical interlocking in providing a friction-based resistance to shear, which is less susceptible to the thermal impacts than the binder's adhesive bond. Quantitatively, this contribution is reflected in the substantial positive coefficient of +51.44, confirming that mechanical interlock provides a robust shear resistance independent of the binder's state.

Table 6- Summary of the initial regression model

Parameter	Coefficient	P-value	Parameter	Coefficient	P-value
(Intercept)	488.8089	0	Temperature * Geocomposite	-0.8353	0.184
Temperature	-11.6655	0	Confinement Load * Tack Coat Rate	0.2267	0.169
Confinement Load	0.6136	0	Confinement Load * Surface Preheating	-0.0696	0.394
Tack Coat Rate	57.9942	0.268	Confinement Load * Aggregate Interlock	0.022	0.787
Surface Preheating	43.6941	0.242	Confinement Load * Geocomposite	-0.111	0.178
Aggregate Interlock	36.6391	0.325	Tack Coat Rate * Surface Preheating	-32.5999	0.384
Geocomposite	43.745	0.241	Tack Coat Rate * Aggregate Interlock	-2.0202	0.957
Temperature * Confinement Load	0.0006	0.811	Tack Coat Rate * Geocomposite	-27.3948	0.464
Temperature * Tack Coat Rate	0.3884	0.755	Surface Preheating * Aggregate Interlock	1.0597	0.955
Temperature * Surface Preheating	-0.007	0.991	Surface Preheating * Geocomposite	5.6223	0.763
Temperature * Aggregate Interlock	0.3789	0.543	Aggregate Interlock * Geocomposite	-27.0591	0.152

Table 7- Summary of the final optimized regression model

Parameter	Coefficient	Std. Error	t-statistic	P-value
Intercept	547.0797	10.665	51.295	0
Temperature	-11.5318	0.296	-38.985	0
Confinement Load	0.4304	0.091	4.735	0
Aggregate Interlock	51.4385	10.868	4.733	0
Confinement Load * Tack Coat Rate	0.387	0.11	3.531	0.001
Aggregate Interlock * Geocomposite	-34.6366	12.55	-2.76	0.008
Model Summary				
R-squared: 0.97	F-statistic: 380.1		Prob (F-statistic): 5.66E-43	

Additionally, confinement load also provides a significant positive contribution. This effect is attributed to the increased normal force across the interlayer, which enhances the frictional resistance through aggregate interlock. This physical enhancement is reflected in the model by the positive coefficient of +0.43, indicating a direct linear contribution to shear resistance. Regarding interaction effects, a significant positive interaction between confinement load and tack coat rate is observed, indicating that the benefit of a higher tack coat rate is amplified under higher confinement loads. This can be interpreted as the confinement load ensuring more contact between the asphalt layers, which allows the higher tack coat to be more effective in creating a stronger adhesive bond. Statistically, this synergistic behaviour is captured by the positive interaction coefficient of +0.387.

Another striking point is the significant negative interaction between aggregate interlock and the geocomposite ($p = 0.008$). The model shows that while aggregate interlock has a positive effect, the simultaneous presence of a geocomposite introduces a negative interaction term of -34.64 kPa. This is consistent with the hypothesis that the geocomposite textile can act as a layer, preventing the full friction between layers. This finding mathematically explains why in some cases a geocomposite-reinforced structure with interlock did not perform as well as might be expected.

Although some specific experimental configurations in this study suggested a potential interaction between the tack coat application rate and the presence of a geocomposite, this interaction term was not statistically significant in the final optimised multivariable regression model. The backward elimination process revealed that the above-mentioned dominant factors overshadowed the influence of this interaction. The ISS values predicted by Equation (1) were plotted against the actual experimental values obtained in the laboratory in Fig. 7.

To provide a rigorous statistical evaluation, the plot includes both the 95% Confidence Interval (CI), represented by the orange shaded region, and the 95% Prediction Interval (PI), shown in the blue

shaded region. CI represents the uncertainty in the model's mean prediction, and, as observed, the CI band is narrow, demonstrating the model's high precision in estimating the mean response. Furthermore, the blue band indicates the range where individual experimental observations are expected to fall. The fact that most data points lie within the Prediction Interval, combined with the high R^2 of 0.97, confirms the model's robustness.

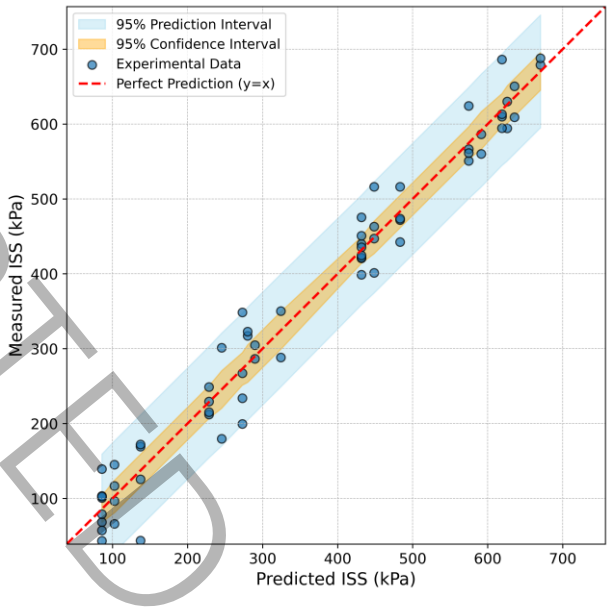

Fig. 7. Comparison of measured vs. predicted ISS values from the final model

To ensure the statistical validity of the optimised regression model, the underlying assumptions, including normality, homoscedasticity, and independence of errors, were verified. Fig. 8 illustrates the diagnostic plots for the residual analysis. As shown in the Normality Check (Histogram and Q-Q Plot), the residuals closely follow the theoretical normal distribution and align with the diagonal line. This visual inspection is statistically corroborated by the Jarque-Bera test (P-value = 0.955) and the Omnibus test (P-value = 0.803), both of which fail to reject the null hypothesis of normality, confirming the Gaussian distribution of errors. Furthermore, the Homoscedasticity Check (Residuals vs. Fitted values) displays a random scatter of points around the zero line without any distinct patterns (e.g., funnel shape), validating the assumption of constant variance. Finally, the Independence Check confirms the absence of autocorrelation among residuals, a finding further supported by the Durbin-Watson statistic of 2.274, which falls within the acceptable range (1.5–2.5). Collectively, these diagnostics confirm that the model assumptions are fully met and the regression results are statistically robust.

Finally, to provide a visual representation of the final predictive model, contour plots were generated, as shown in Fig. 9. Each plot illustrates the predicted ISS as a function of confinement load and tack coat rate. Several critical findings can be visually confirmed from this figure. Firstly, the strong negative effect of temperature is evident by the significant drop in ISS values when moving down the rows. Secondly, a comparison across the columns clearly demonstrates the hierarchy of the structural enhancements; the third column (Aggregate Interlock: 1, Geocomposite: 0) consistently shows the highest ISS values, while the second column (Aggregate Interlock: 0, Geocomposite: 1) shows the lowest, confirming the dominant positive effect of interlock and the negative main effect of the geocomposite. Most importantly, the curvature and spacing of the contour lines visualise the significant interaction effects. The non-parallel lines illustrate the synergistic relationship between confinement load and tack coat rate.

Furthermore, the visible reduction in overall strength when comparing the fourth column to the third provides an explicit visual confirmation of the negative interaction term (interlock×Geocomposites), quantifying the trade-off inherent in using this reinforcement method.

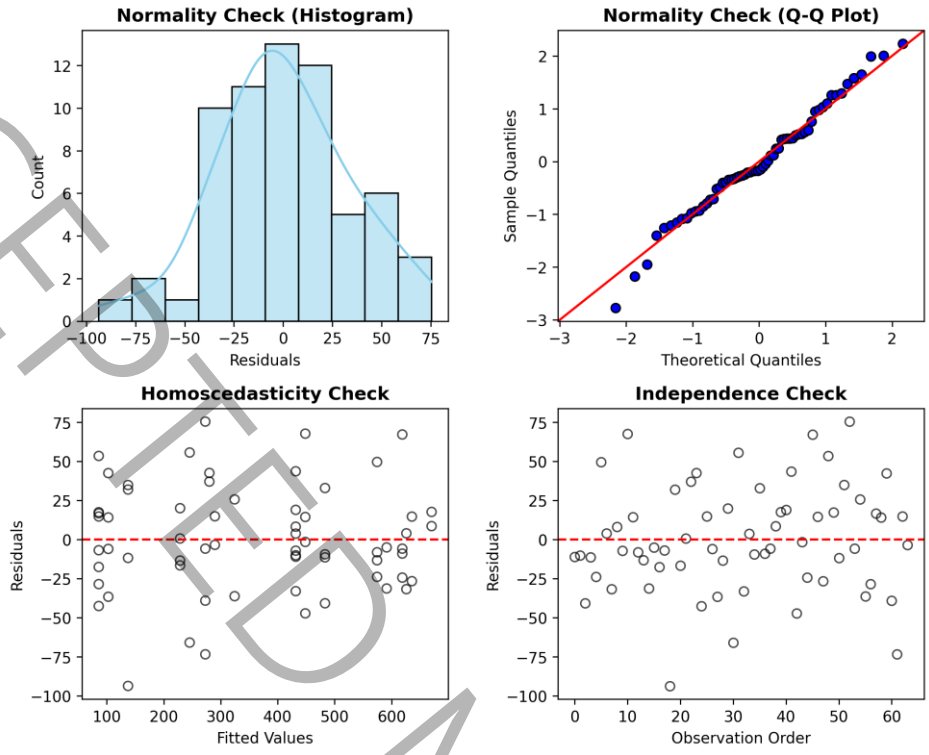

Fig. 8. Verification plots of regression model assumptions: Normality, Homoscedasticity, and Independence

4 Study Limitations

While the use of a single material type was necessary to isolate the interaction effects and eliminate confounding variables, as detailed in the Materials section, it is essential to acknowledge that the quantitative results may vary for different materials. Moreover, the environmental conditions were simulated at discrete temperatures, but in-service pavements experience continuous thermal cycles that were not fully replicated. Additionally, although the AUT-SLT device effectively simulates shear loading and provides precise control over variables, there may be differences between laboratory-scale and full-scale testing.

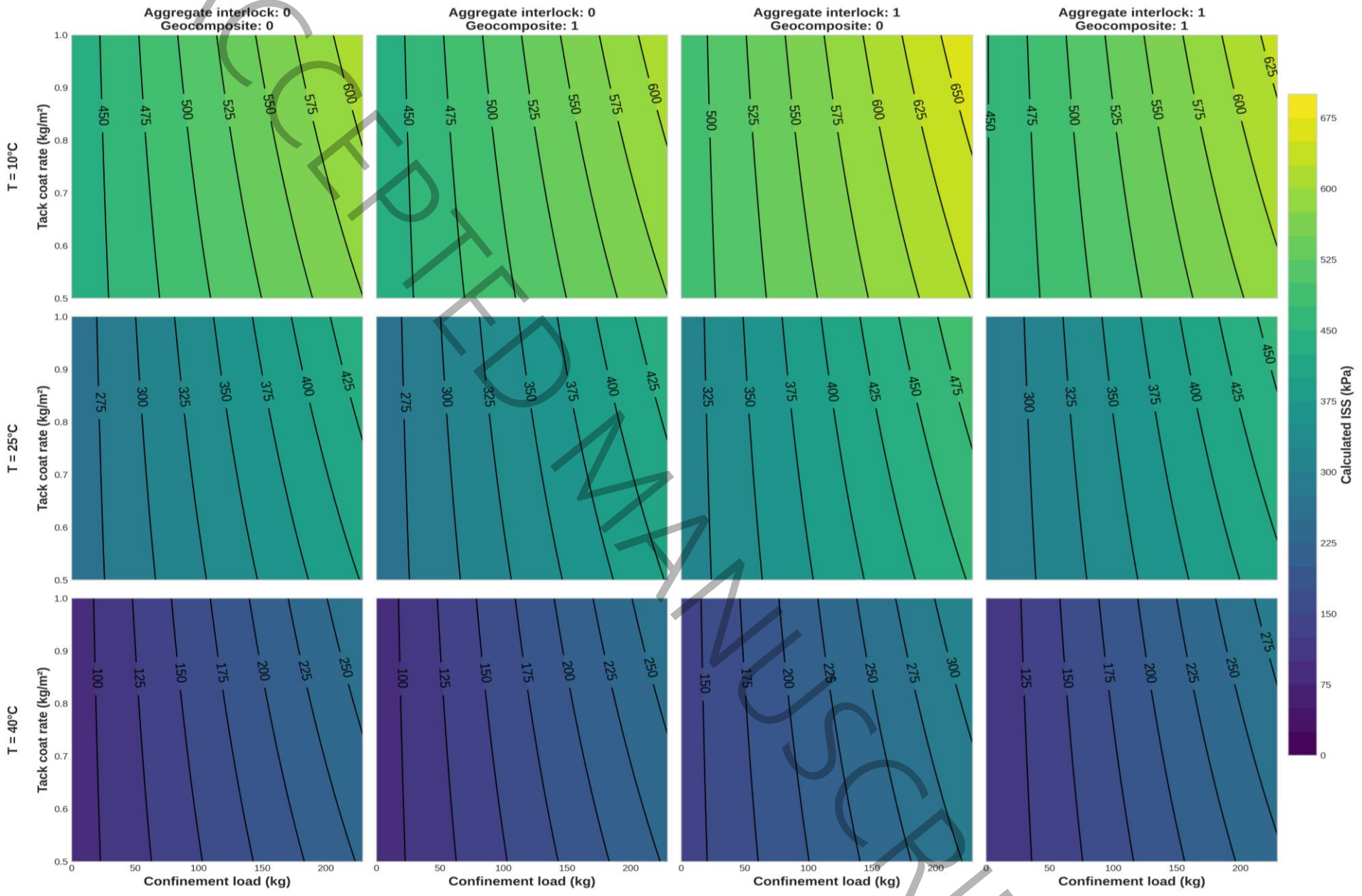

Fig. 9. Contour plots of predicted ISS as a function of confinement load and tack coat rate at three temperatures 10°C, 25°C 40°C

5 Conclusions

This study conducted experimental and statistical analyses to assess the effects of temperature, tack coat application rate, geocomposites, confinement load, preheating, and aggregate interlocking on the bonding properties of AC layers. The following conclusions can be summarized:

- Temperature was the most detrimental factor. An increase from 10°C to 40°C reduced the overall average strength by more than 2.5 times. Conversely, the mechanical contributions of aggregate interlock and confinement load proved to be the most reliable methods for enhancing ISS. Aggregate interlock boosted strength by 28% at 40°C, while a 229 kg confinement load increased the average ISS by 60% compared to the zero-load condition.
- The contribution of surface preheating was statistically negligible. Its main effect was found to be insignificant in the final regression model, and it was ultimately removed during the backward elimination process.
- While a higher tack coat rate generally improves ISS, its main effect was not statistically significant in the final optimised model. Instead, its benefit was primarily captured through a powerful synergistic interaction with confinement load, which was highly significant.
- The use of a geocomposite was generally detrimental to ISS. Also, the final regression model revealed a significant negative interaction between aggregate interlock and the geocomposite. This indicates that the geocomposite can partially counteract the mechanical benefits of an interlocked surface.
- Ultimately, this study demonstrates that designing a durable pavement interlayer is not merely about adding individual enhancements, but about creating a compatible and synergistic system. Simply deploying a geocomposite or increasing tack coat dosage without considering interaction effects can lead to suboptimal results. Translating these laboratory findings into practice requires a holistic approach that addresses specific implementation challenges. While geocomposites are essential for delaying reflective cracking, they present a critical trade-off by potentially compromising interlayer shear strength if not properly managed. Consequently, engineers must balance these factors by adopting comprehensive measures such as ensuring wrinkle-free installation, maintaining surface cleanliness, and utilising surface milling to maximise aggregate interlock. This integrated strategy, which accounts for both material interactions and construction realities, is essential for ensuring that the pavement structure can withstand complex loading and environmental stresses in the field.

To enhance the comprehensiveness of this study, future research should investigate dynamic loading protocols and moving load effects to better capture the viscoelastic response of the interlayer under realistic traffic conditions. Additionally, the experimental scope should be broadened to evaluate various asphalt mixture types with different aggregate gradations and material compositions, ensuring the findings are applicable to a wider range of pavement structures. Further studies are also recommended to validate these laboratory results through full-scale field testing or Accelerated Pavement Testing (APT), as well as to examine the impact of different tack coat types (e.g., polymer-modified) and environmental factors such as freeze-thaw cycles on long-term durability.

References:

[1] A. Collop, M. Sutanto, G. Airey, R. Elliott, Shear bond strength between asphalt layers for laboratory prepared samples and field cores, Construction and Building Materials, 23(6) (2009) 2251–2258.

[2] M. Diakhaté, A. Millien, C. Petit, A. Phelipot-Mardelé, B. Pouteau, Experimental investigation of tack coat fatigue performance: Towards an improved lifetime assessment of pavement structure interfaces, Construction and Building Materials, 25(2) (2011) 1123–1133.

[3] B. Al Hakim, L.W. Cheung, R.J. Armitage, Use of FWD data for prediction of bonding between pavement layers, International Journal of Pavement Engineering, 1(1) (1999) 49–59.

[4] C. Raab, M.N. Partl, Interlayer bonding of binder, base and subbase layers of asphalt pavements: Long-term performance, Construction and Building Materials, 23(8) (2009) 2926–2931.

[5] L. Tashman, K. Nam, T. Papagiannakis, K. Willoughby, L. Pierce, T. Baker, Evaluation of construction practices that influence the bond strength at the interface between pavement layers, Journal of Performance of Constructed Facilities, 22(3) (2008) 154–161.

[6] W. Zhang, Effect of tack coat application on interlayer shear strength of asphalt pavement: A state-of-the-art review based on application in the United States, International Journal of Pavement Research and Technology, 10(5) (2017) 434–445.

[7] E.S. HARIYADI, K.P. AURUM, B.S. SUBAGIO, Theoretical Study of Bonding Condition at the Interface between Asphalt Pavement Layers, Journal of the Eastern Asia Society for Transportation Studies, 10 (2013) 1590–1597.

[8] H.M. Al-Mosawe, N. Thom, A Comprehensive Review of Interlayer Bond Strength in Asphalt Pavement Systems, Al-Rafidain Journal of Engineering Sciences, (2025) 155–175.

[9] M.Y. Shahin, E.W. Blackmon, T. Van Dam, K. Kirchner, Consequence of Layer Separation on Pavement Performance, 1987.

[10] L.N. Mohammad, M. Raqib, B. Huang, Influence of asphalt tack coat materials on interface shear strength, Transportation Research Record, 1789(1) (2002) 56–65.

[11] X. Hu, Y. Lei, H. Wang, P. Jiang, X. Yang, Z. You, Effect of tack coat dosage and temperature on the interface shear properties of asphalt layers bonded with emulsified asphalt binders, Construction and Building Materials, 141 (2017) 86–93.

[12] D. Hou, M. Han, Y. Muhammad, Y. Liu, F. Zhang, Y. Yin, S. Duan, J. Li, Performance evaluation of modified asphalt based trackless tack coat materials, Construction and Building Materials, 165 (2018) 385–394.

[13] R. Ghabchi, M.M. Zaman, S. Rani, Development Of Guidelines For Selection And Evaluation Of Tack Coats In Oklahoma, (2018).

[14] D. Covey, E. Coleri, A. Mahmoud, Tack coat rheological properties and the effects on interlayer shear strength, Journal of Materials in Civil Engineering, 29(11) (2017) 04017221.

[15] M.R. Kruntcheva, A.C. Collop, N.H. Thom, Properties of asphalt concrete layer interfaces, Journal of Materials in Civil Engineering, 18(3) (2006) 467–471.

[16] A. Raposeiras, D. Castro-Fresno, A. Vega-Zamanillo, J. Rodriguez-Hernandez, Test methods and influential factors for analysis of bonding between bituminous pavement layers, Construction and Building Materials, 43 (2013) 372–381.

[17] A. Bae, L.N. Mohammad, M.A. Elseifi, J. Button, N. Patel, Effects of temperature on interface shear strength of emulsified tack coats and its relationship to rheological properties, Transportation research record, 2180(1) (2010) 102–109.

[18] A. Noory, F. Moghadas Nejad, A. Khodaii, Evaluation of shear bonding and reflective crack propagation in a geocomposite reinforced overlay, Geosynthetics International, 24(4) (2017) 343–361.

[19] V.V. Kumar, G.H. Roodi, J.G. Zornberg, Evaluation of geosynthetic-asphalt interface characteristics using Leutner shear tester, in: Geosynthetics: Leading the Way to a Resilient Planet, CRC Press, 2023, pp. 2146–2152.

[20] N.S. Correia, T.R. Souza, M.P. Silva, V.V. Kumar, Investigations on interlayer shear strength characteristics of geosynthetic-reinforced asphalt overlay sections at Salvador International Airport, Road Materials and Pavement Design, 24(6) (2023) 1542–1558.

[21] N.S. Correia, A.L.C. Souza, K.M. Dos Santos, V.V. Kumar, Fatigue performance of geosynthetic-reinforced asphalt using DIC, in: E3S Web of Conferences, EDP Sciences, 2024, pp. 02005.

[22] N. Sudarsanan, A. Arulrajah, R. Karpurapu, V. Amrithalingam, Fatigue performance of geosynthetic-reinforced asphalt concrete beams, Journal of Materials in Civil Engineering, 32(8) (2020) 04020206.

[23] S. Spadoni, L.P. Ingrassia, G. Paoloni, A. Virgili, F. Canestrari, Influence of geocomposite properties on the crack propagation and interlayer bonding of asphalt pavements, Materials, 14(18) (2021) 5310.

[24] J.-S. Chen, C.-C. Huang, Effect of surface characteristics on bonding properties of bituminous tack coat, Transportation research record, 2180(1) (2010) 142–149.

[25] X. Yang, A. Rahman, Y. Luo, Y. He, X. Li, C. Ai, Effects of interlayer surface characteristics on the interface bonding between double-layered asphalt systems, International Journal of Pavement Engineering, 24(1) (2023) 2192496.

[26] R. West, Evaluation of bond strength between pavement layers, NCAT report, (2005).

[27] K. Yang, R. Li, Characterization of bonding property in asphalt pavement interlayer: A review, Journal of Traffic and Transportation Engineering (english edition), 8(3) (2021) 374–387.

[28] D. Yin, L. Wang, L. Yin, Z. Wang, S. Liu, L. Li, Torsional Shear Resistance of Pavement Structure with Rubber Powder–Modified Asphalt Gravel Bonding Layer, Journal of Materials in Civil Engineering, 37(4) (2025) 04025032.

[29] A. Noory, F. Moghadas Nejad, A. Khodaii, Evaluation of the effective parameters on shear resistance of interface in a geocomposite-reinforced pavement, International Journal of Pavement Engineering, 20(9) (2019) 1106–1117.

[30] A. Noory, F.M. Nejad, A. Khodaii, Effective parameters on interface failure in a geocomposite reinforced multilayered asphalt system, Road Materials and Pavement Design, 19(6) (2018) 1458–1475.

[31] C. Lung, M. Mohd Hasan, M. Hamzah, A. Sani, S. Poovaneshvaran, P. Ramadhansyah, Effect of temperatures and loading rates on direct shear strength of asphaltic concrete using layer-parallel direct shear test, in: IOP Conference Series: Materials Science and Engineering, IOP Publishing, 2020, pp. 012047.